Journal Pre-proof

Application of Portable Streamer Traps for obtaining Point Measurements of Total Longshore Sediment Transport Rates in Mixed Sand and Gravel Beaches

Andres Payo[1*], Humphrey Wallis[2], Michael A. Ellis[3], Andrew Barkwith[4], Timothy Poate[5]

[1]Andres Payo, PhD, Senior Scientist, British Geological Survey, Keyworth, NG12 5GG, UK; agarcia@bgs.ac.uk [*]Corresponding Author

[2]Humphrey Wallis, Senior Engineer, British Geological Survey, Keyworth, NG12 5GG, UK; hcw@bgs.ac.uk

[3]Michael A. Ellis, PhD, Senior Scientist, British Geological Survey, Keyworth, NG12 5GG, UK; mich3@bgs.ac.uk

[4]Andrew Barkwith, PhD, Senior Scientist, British Geological Survey, Keyworth, NG12 5GG, UK; andr3@bgs.ac.uk

[5]Timothy Poate, PhD, Senior Scientist, CMAR, Plymouth, Devon, PL4 8AA, UK; timothy.poate@plymouth.ac.uk

Journal Pre-proof

Journal Pre-proof

ABSTRACT

Observations of the depth integrated and time averaged sediment transport on a mixed sand and gravel (MSG) beach are presented and analyzed to examine the performance of a new portable streamer trap. Measurement of the longshore sediment transport rate in the surf zone remains one of the great challenges in coastal engineering and coastal sciences. Sediment traps for sand beaches have proven useful in the past, but are not suitable for MSG beaches. This paper describes a portable depth-integrated streamer trap designed to measure the depth-integrated combined bed load and suspended longshore sediment transport on MSG beaches. The device consists of a polyester sieve cloth mounted into a rectangular holding frame. The stability of the device is achieved by gravity: the combined weight of the device and the operator, who is standing on and down-current of the device. The device has been tested in the field under moderate wave conditions at Minsmere, UK. We show that the observed suspended and bed load sediment transport are proportional to the wave energy flux, as formulated in the standard theoretical model, CSHORE. The data suggest that the empirical efficiency of wave breaking and bed load parameter are several orders of magnitude larger than that previously observed for uniform fine sand values.

ADDITIONAL INDEX WORDS: *Sand transport, gravel transport, measurement technique.*

Journal Pre-proof

Journal Pre-proof

1 INTRODUCTION

Gravel and mixed sand-gravel (MSG) shorelines are common in previously para-glaciated coastal regions and are globally widespread [1]. MSG shorelines are also found where nourishment projects are employed that use sediment size of coarser size than native sediment to protect eroding beaches [2; 3]. Using coarser than native sediment results in steeper beach profiles that require less volume of sand to achieve a given beach width. Coarser sediment is also more stable in terms of longshore losses. Despite their worldwide distribution and the growing interest in beach nourishment as an adaptation strategy for combating coastal erosion [4], sediment transport on MSG beaches is less well understood than on sandy beaches [5]. One of the key elements in improving the engineer's understanding of beach morphodynamics and sediment budgeting along a MSG coastline is the formulation of a reliable estimate of the total longshore transport rate for feasibility studies of port extensions and appraisals of long-term beach stability. Such estimates should be based on the use of reliable sediment transport models, underpinned by accurate transport measurements. However, field sediment transport-rate data, collected simultaneously with waves and currents that drive sediment transport on MSG beaches, are still very limited.

The portable Streamer Trap (ST) described by Kraus [6] is one of the few reliable field measurement techniques available to measure the combined bed load and suspended longshore sediment transport at a given point within the surf zone. The ST consists of long rectangular bags of polyester-sieve cloth material (100 μm) vertically mounted on a stainless steel rack. An operator standing down-current attends the trap during a sampling interval of about 10 min. The use of these traps is restricted to shallow water (<1 m) with wave heights less than about 0.5 m. Researchers have used STs mostly to measure sand sediment transport [6-11], with only one reported use on an MSG beach [12]. Dawe [12] has shown that Kraus' ST design is operationally effective in the swash zone of the MSG shoreline at Lake

Journal Pre-proof

Coleridge, New Zealand. The ST was able to stand unattended for most of the 500 hours measured, where wave heights averaged 0.20 m to 0.35 m, wave periods were 1.43 s to 2.33 s and water depth was 0 m to 0.5m. Most commonly, the trap was in place between 1 min to 5 min. The weight of material collected in the trap ranged from as little as 0.1 kg though to 5.5 kg, with a sediment size variation of between 1 mm to 10 mm (d50).

Chadwick [13] conducted seven successful trapping experiments at Shoreham, UK, using a different sediment trap design than the suggested by Kraus [6], registering transport rates from 4 to 32 m^3/day for waves of between 0.23 and 0.48 H_{rms} and d50 of 20 mm. The surface mounted shingle trap used by Chadwick [13] consists of a right triangular prism frame where all faces except the top (which was open), were made of a mesh that allows the water to flow through and trap the coarse material. The frame is orientated to trap longshore sediment transport (i.e. need to anticipate the main direction of the longshore sediment transport) and is anchored to the ground with pins. The trap is left unattended during a full tidal cycle (i.e. several hours). Bray et al. [14] found that the trap design used by Chadwick was difficult to secure in loose shingle and, therefore, few measurements could be made in areas where sediment mobility was highest. Overall, they found that the trap volumes were several orders of magnitude lower than measured by tracers. They attributed these differences on trapped volumes due to scouring, build-up against the sides of the trap, and loss of material on the ebb tide. They concluded that surface mounted shingle traps are unreliable in conditions other than near-calm.

In this study, we present a new portable streamer trap to measure point-depth-integrated longshore sediment transport on MSG beaches. The aim of this work is to investigate the field performance of the device under moderate wave conditions (i.e. wave heights less than 1 m). To test the performance of the device, we compare measured to simulated rates using the depth-integrated and wave averaged cross shore numerical model CSHORE [15]. During the

Journal Pre-proof

experiment, offshore wave forcing was measured by a directional wave buoy located about 4 km seaward of the study site. Current velocity and water levels were measured with an Acoustic Doppler Velocimeter (ADV) and a pressure sensor anchored to a fixed rig, which was well within the surf zone during the full tidal cycle. A pressure sensor was also attached to the portable streamer trap to provide information relative to water depth and water surface elevation at the trap location.

This paper begins with a detailed description of the limitations of Kraus' ST when used on MSG beaches, and how the new proposed portable Depth Integrated ST (DIST) is designed to minimize some of these limitations. We then present the study site, the MSG beach at Minsmere, Suffolk, UK. Within the methodology section, we present the experimental and numerical setup. In particular, we describe the field setup of the auxiliary instruments used to characterize the drivers of longshore sediment transport and the main assumptions, formulation and inputs used for the numerical simulation of the longshore sediment transport using the CSHORE model. Subsequently, in the results section, we show that the measured suspended sediment rates compare well with the simulated CSHORE results, suggesting that the traps were effectively capturing the longshore sediment transport. We also show how the CSHORE formulation for longshore bed load sediment transport, which has never been validated with field data, seems to be in good agreement with the observations. We conclude with some recommendations for future work and main lessons learned from this experiment.

2 DEPTH-INTEGRATED STREAMER TRAP

2.1. Limitations of streamer traps when applied to mixed sand and gravel beaches

General descriptions of the limitations of Kraus' ST design have been published elsewhere [6; 8; 12; 16; 17]. In this section, we describe the specific limitations of using Kraus' ST on

Journal Pre-proof

MSG beaches. The authors would like to note that we are interested in the depth-integrated longshore sediment transport or the vertical distribution of sediment transport. Our ultimate goal is to support the development of reliable longshore sediment transport formulations and, for this purpose, depth-integrated formulations may require fewer assumptions and empirical parameters than those that resolve the vertical distribution. Kraus' STs were designed to measure sediment transport rates at a number of discrete vertical locations. To obtain the vertically integrated longshore sediment transport, users are forced to either interpolate [17] or fit the best vertical distribution and integrate the fitted distribution over depth [6]. Fitting the best vertical distribution to vertically-discrete sediment transport measurements is both time consuming and error prone [i.e. 18], and should be avoided when possible.

The streamer trap concept, was originally designed by Katori [19] to measure longshore sand transport in the surf zone and expressly designed to mitigate some of the common problems associated with traditional trap designs, namely bed scour and current flow interference. Based on observations during use in the field, the ST produces relatively minor scour as compared with bulkier traps, if the sampling interval is sufficiently short (less than approximately 5 to 10 minutes) [6]. Rosati and Kraus [17] analysed the hydraulic and sand trapping efficiency of the streamer trap nozzle for use in the nearshore zone and also recommended that testing periods do not extend beyond the 5 to 10 minute interval to avoid scouring problems.

Keeping STs in position during observation periods on MSG beaches is more challenging than on sandy beaches. On sandy beaches, the ST is anchored to the bottom by thrusting the back legs of the frame into the bed [6], however, use of a similar method for MSG is often not possible or, when possible, it will take the order of minutes to anchor it creating scouring problems. Additionally, on MSG beaches, energy dissipation through wave-breaking is concentrated over a much narrower region than on a sandy beach (i.e. plunging wave

Journal Pre-proof

136 breaking is more likely to occur on steep slopes and moderate wave conditions rather than
137 spilling breaking mode), making it more difficult to keep the ST in place.

138 The proposed DIST device is a modification of the ST design described by Kraus [6]. It has
139 been adapted to measure the depth-integrated total sand and gravel longshore sediment
140 transport, whilst mitigating the limitations mentioned above (i.e. depth integrated
141 measurement instead of vertically discrete observations, scouring and trap efficiency,
142 anchoring).

143

144 **2.2. New streamer trap proposed design**

145 The DIST is made of a stainless steel rectangular mouth (1,000 mm height x 250 mm wide x
146 100 mm deep) with four welded ring clamps (two at vertical side) that slide onto two stainless
147 steel cylindrical tubes (1,250 mm height x 25 mm diameter) (Figure 1). The tubes are
148 anchored to a square base (1,000 mm span x 1,000 mm length and a mesh of 30 mm x 30mm)
149 that provides grip and a stable surface on which the operator is standing during the
150 observation period. For economy, the reticulated base is made of commercially available
151 galvanized grating panels on the standard N grating with edges. The standard N grating,
152 comprising equal height bars in both directions, provides both strength and maximum weight-
153 to-surface ratio. The rectangular frame is further secured to the base by two additional
154 stainless steel bracing tubes (25 mm diameter) that connect the vertical poles with the corners
155 of the rectangular base. The anchoring points to the base are made of two articulated
156 components allowing the bracing tubes to be easily assembled to the base at the correct angle.
157 All the components of the streamer trap, apart from the rectangular base, are marine grade
158 stainless steel, giving maximum resistance to corrosion.

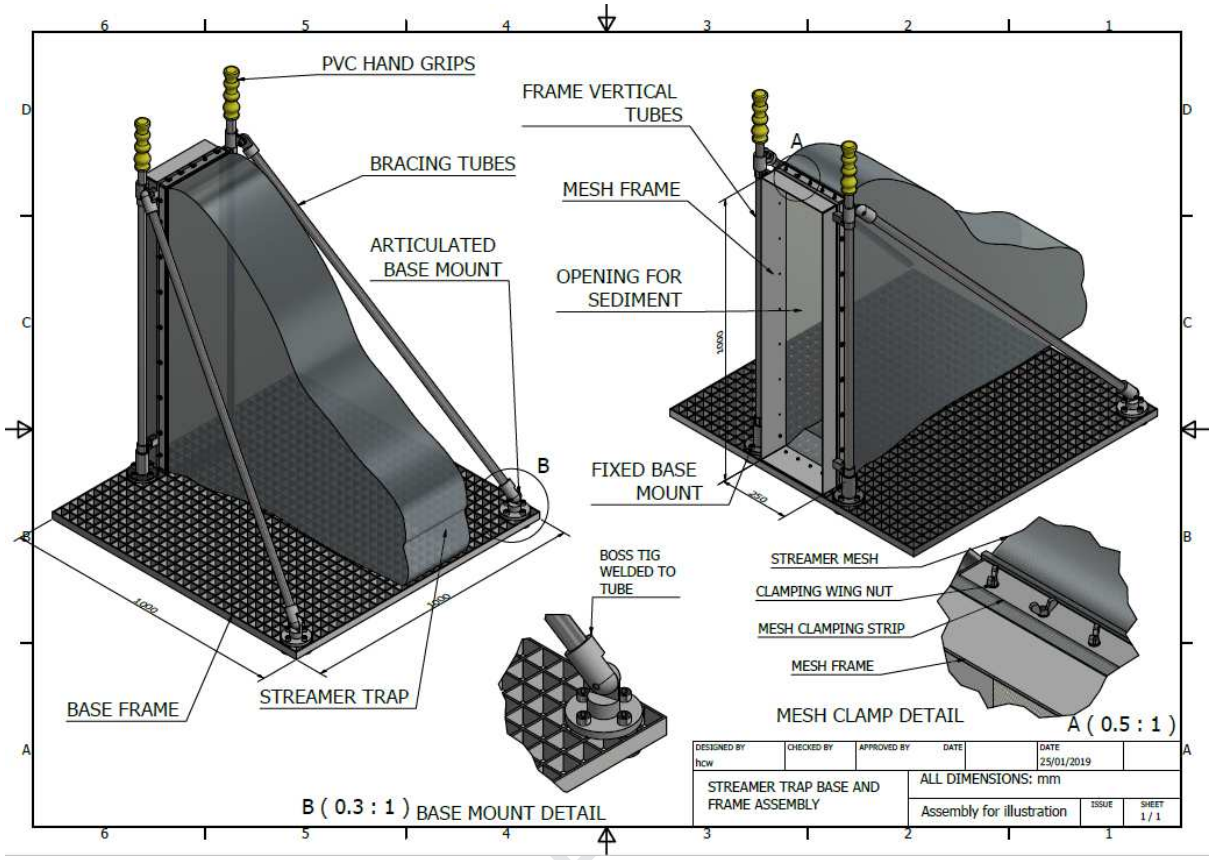

Figure 1. Total Streamer Trap holding frame and streamer.

The streamer is made of 1.5 m^2 of polyester sieve cloth (0.105 mm mesh), used to trap sediment from sand to gravel size (125 µm to 64 mm). (Material larger than 64 mm will also be trapped, but can be easily removed, and in any case is extremely rare.) The sieve cloth has been shaped and sewn as an oblique rectangular pyramid (1,000 mm height), with a base of slightly larger dimensions than the streamer mouth (i.e. to be able to fit the streamer to the mouth), and the apex aligned with the center of one of the shorter sides of the rectangular base. The opening of the streamer that connects with the rectangular mouth is reinforced with a canvas hem. The streamer is mounted into the rectangular mouth frame with the plane made by the apex and the apex-aligned shorter side of the rectangle at the bottom. Streamer frames are secured on the rectangular mouth by bearing pressure created by stainless steel plates on each side of the mouth. Locking pressure is achieved by tightening a number of wing nuts

Journal Pre-proof

along each side of the frame. The device has been designed to be quickly assembled and dismantled in the field.

2.3 Operation

To begin a cycle of use, the streamer is mounted in the holding frame and secured using a number of stainless steel bolts. The total weight of the DIST is 42.6 kg and can be transported and recovered by two people (Figure 2a). The trap is positioned in the surf-zone with the streamer mouth facing the longshore current (Figure 2b). The operator stands on the reticulated base, behind the streamer and holding the handles at the top of the vertical poles. The device is held stable by both gravity (i.e. weight of the device plus the weight of the operator) and the grip provided by the reticulated base, which buries itself into the bed after the first few waves have passed and under the weight of the operator. At the end of the sampling interval, typically 5 to 10 min, the trap is brought back to shore (Figure 2c) and the collected sediment is transferred from the streamer to a container (Figure 2d). Once the sediment is transferred, the device is ready to start a new observation.

Journal Pre-proof

Figure 2. Photograph showing traps in operation: (a) transportation from dry beach to sampling location; (b) during sampling one operator holds trap in place by standing on top of the reticulated base; (c) once sampling is finished, two people recover the trap and (d) transfer the collected sediment to a bucket first and a labelled plastic bag for storing and sediment size analysis.

3 STUDY SITE

3.1. Location and Lithology

The study area lies on the East coast of England at Minsmere Cliffs, located between Dunwich and Sizewell (Figure 3).

Site lithology (see Figure 3) consists of bedrock overlain by superficial deposits on land and by a sediment layer on the seabed. The geology of the inland area between Southwold and Aldeburgh consists mainly of Crag deposits (Pliocene and Pleistocene in age) and weakly cemented sedimentary rocks, notably the Coralline Crag Formation (Calcarenite) that outcrops near Aldeburgh. The Crag deposits are mainly shallow marine, coastal, and estuarine in origin, and made of sands, gravels, silts and clays. The sands are characteristically dark green when freshly exposed (glauconite present) but weather to a bright orange color (hematite present). The gravels in the lower part of the group are almost entirely composed of flint. Minsmere Cliffs are mostly un-lithified gravel deposits and the beach deposits are mostly sand (grain size between 0.063 mm and 2.0 mm) and gravel (grain size between 2.0 mm to 63 mm). South of Minsmere cliffs there are areas of lowland with patches of peat, diamicton-rich (i.e. sediments that are poorly sorted and contain a wide range of clast sizes) superficial deposits, and sand bedrock deposits.

The seabed layer, from the coastline to about 4 km seaward (i.e. the nearshore), consists mostly made of sand and muddy-sand, while the offshore seabed sediment layer consists mostly of coarser sediments. Sand and muddy-sand are defined here as an amalgamation of sand and slightly gravelly sand classes (as defined by the Folk classification [20]), and those parts of the muddy-sand and slightly gravely-muddy-sand classes where the mud to sand ratio is less than 1 to 4. Coarse sediments are defined as an amalgamation of the gravel, sandy-gravel, gravelly-sand and classes as defined by the Folk classification [20].

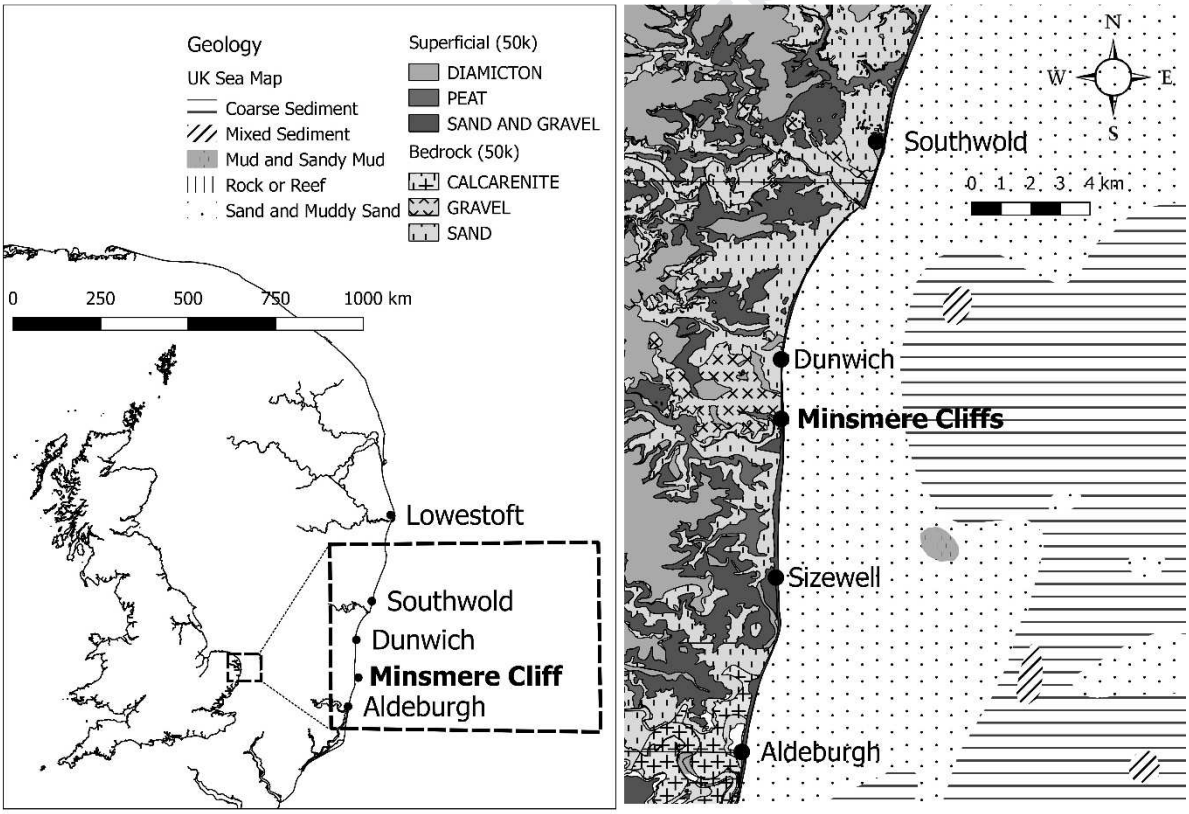

Figure 3. Location of the study area, showing the main locations referred to in the text and the lithology of the area.

3.2. Bathymetry, tides, winds, waves and storm surges

223 The beach profile and meteo-oceanographic conditions were measured during the field
224 experiment, and only a brief summary is provided here to complete the overall study area
225 description. The information summarized here has been extracted from the more detailed
226 description of bathymetry, tides, winds, waves and storm surges provided by Pye and Blott
227 [21]. Tides at the study site are semidiurnal, with the level of predicted high waters relative to
228 Ordnance Datum (OD) reaching a minimum near the Minsmere Cliff (*ca.* 0.8m OD at springs
229 and *ca.* 0.4 m OD at neaps). Tidal current residual flows of the Dunwich-Sizewell coast are
230 very small and directed southwards. The maximum residual flow reaches 0.05 m s^{-1} over
231 Dunwich Bank and near the shore along the Dunwich cliffs. Elsewhere, residual flows are
232 less than 0.05 m s^{-1}. Records from 1981 to 2000 show that the prevailing winds blow from
233 the southwest, Aeolian sand transport along the shoreline occurs only when winds blow from
234 the north-easterly, easterly or south-easterly directions.

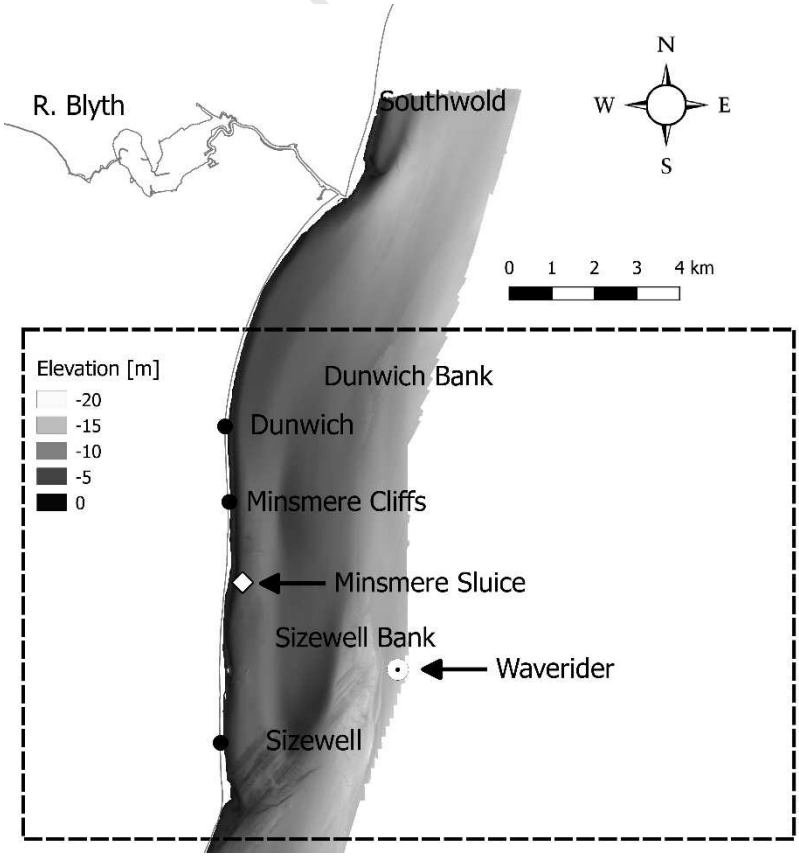

235

Journal Pre-proof

Figure 4. Bathymetry of the study area (based on UKHO bathymetry data: 2017 HI1495 Orford Ness to Southwold Area 4 1m CUBE). Locations of the Sizewell wave rider buoy and Minsmere Sluice (tidal data) shown as a circle and diamond, respectively.

No long-term measured inshore wave records are available for this coast, although wave recorders have been deployed at several locations for short periods at varying times [21]. The Sizewell wave rider buoy located *ca.* 4 km offshore of Sizewell was operative during the field experiment (Figure 4). Wave conditions registered at the Sizewell buoy are bi-directional from the northeast and south. Typical winter waves reach 0.5 to 1.0 m with 7.0 s peak period. The importance of the Dunwich and Sizewell Banks (Figure 4) in reducing wave energy reaching the coast has been a matter of some debate [21], and it is concluded that although the banks might have little influence on waves at the shoreline during typical weather conditions, they may be far more important in sheltering the coast during storms (i.e. wave height >2.0 m). Because the astronomical tidal range is small along this part of the coast, surges can have a proportionately large impact on the resultant tidal levels. The storm of 31 January 1953 produced the largest surge recorded, and resulted in the highest tide levels (3.50 m OD at Southwold and 3.78 m OD at Aldeburgh). Comparison of measured with predicted tidal levels shows that surges of <1 m occur relatively frequently at the study area [21].

4 METHODS

4.1 Field experiment setup

A field experiment involving 21 DIST deployments was carried out from 8th to the 10th January 2018, at the MSG beach in front of the Minsmere Cliff (Figure 5). The point measurements were made within the upper shoreface, where water depth was less than 1 m and it was safe for an operator to stay with the device under breaking waves. The

Journal Pre-proof

approximate locations of the DIST deployments were measured using a lightweight LASER range finder (LTI TruPulse 360). The LASER range finder measures distance, inclination and azimuth, and can calculate horizontal and vertical distances with accuracies of ±30 cm when measurements are made of a high-quality target. An operator standing on the beach on a point of known coordinates (point 0 shown in Figure 5) measured the horizontal distance and azimuth to the DIST location by targeting the bright and highly reflective lifejacket worn by the DIST operator. The coordinates of the DIST location were calculated by translating the known coordinates of the reference point to the observed horizontal distance and azimuth. Three DIST units were used for this field experiment. Two units were operated simultaneously and one kept ashore as spare. For each observation, the device was moved from the dry beach to the desired location with the trap mouth facing the incoming waves and, once in place, rotated to ensure that the trap mouth was facing the longshore sediment transport direction. Sampling at each point was concluded when the maximum sampling period of 10 minutes was reached, or when the trap operator determined that enough sediment had been trapped (i.e. any weight between 0.5 kg to *ca.* 5 kg) The trap operator can roughly assess the amount of sediment trapped by visual inspection of the net when becomes visible between waves.

Three trial deployments were made on day 1 (8^{th} Jan 2018) and 18 on day 2 (9^{th} Jan 2018) under moderate and low stormy conditions, respectively. Day 1 observations were done as a test before the primary observation day when the drivers of longshore sediment transport were also recorded.

We have used three pressure transducers (PT), including two RBR Duo T-Wave PTs at variable locations attached to each trap, and one RBR Solo D-Wave, PT2, at a fixed location logging continuously at 6Hz and 8Hz, respectively. The PTs provide information about the water levels, wave height and wave period at each location.

A Nortek Acoustic Doppler Velocimeter (ADV) was co-located with PT2 on a fixed rig to provide information about cross-shore and longshore currents. The ADV was mounted above the bed on a scaffold "H" frame that provides a stable platform under heavy wave loading. The sensor head was positioned to look down and sample ~0.25 m above the bed, logging continuously at 8Hz. The ADV was fixed 0.4 m above the bed to look downward and measure a sample volume 14.9 mm below the ADV head.

Beach profile elevation change was measured using a Trimble RTK GPS Receiver. The beach profile was measured twice a day during a low tide, extending from the top of the beach to the low water position (Figure 5). RTK GPS surveys were processed to remove any outliers and invalid data points, with coordinates recorded in Eastings and Northings with elevations (m) referenced to ordnance datum Newlyn (ODN).

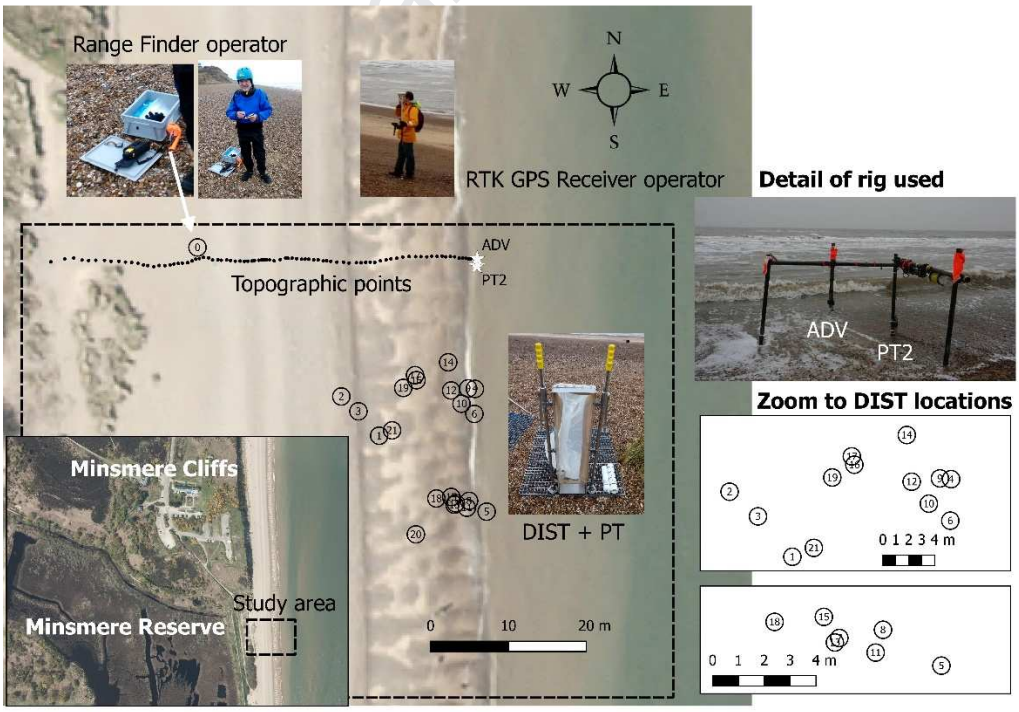

Figure 5. Field experimental set-up. The numbered circles represent the spatial location of the 21 DIST deployments on 8th and 9th January 2018. The circle with number 0, represents

Journal Pre-proof

the reference point used to measure the DIST locations with the LASER range finder. The fixed locations of the ADV and PT2 are represented by a white star symbol. Additionally to the fixed PT2 sensor, a PT sensor was mounted on the DIST base. The black points represent the location of the measured topographic points using an RTK GPS Receiver.

Tidal elevations were obtained from the UK Hydrographic Office astronomical tide projections at Minsmere Sluice as the closest operational tidal gauge to the study site is located at Lowestoft Note: there is a *ca.* 70 minute time lag between high and low tides between Lowestoft and Minsmere Sluice that make tidal levels observed at Lowestoft unrepresentative of the tidal levels during the field experiment. The effects of the barometric tide and wind-stress induced tide on the astronomical tide were included during the data processing.

4.1.1 Data processing

The ADV time series was processed to identify data with a poor signal to noise ratio (SNR) by removing data with <70% correlation and a minimum amplitude of 55. These values are arbitrary and purely based on manual examination of the data signal. Data that is identified as an outlier and in excess of three times the standard deviation (of a one minute data burst) is also replaced by NaNs. These steps are provided as a first order QC process designed to allow initial processing and are not implied to be comprehensive.

We have corrected the offset due to atmospheric pressure changes on the elevation time series from all PTs. The PTs used in this field experiment measure and record total pressure, where total pressure is the sum of atmospheric pressure and sea level pressure. Atmospheric pressure must be removed from total pressure to obtain sea pressure, and sea pressure is

Journal Pre-proof

required to calculate, for example, depth. The PT installed on the spare DIST unit was never submerged and provided a time series of the atmospheric pressure at the study site. The atmospheric pressure decreased from 1005.77 hPa to 1004.69 hPa during the DIST deployments period on (i.e. from 12:50am to 15:30pm January 9th 2018). For each PT the water level signal is computed assuming a reference atmospheric pressure of 1005 hPa as;

$$\textit{Water Level}\ [\mathrm{m}] = (p\ [\mathrm{dbar}] - a\ [\mathrm{dbar}]) / (0.980665\rho\ [\mathrm{g/mL}]) \quad (1)$$

where, p is hydrostatic pressure (in dbar from sensor), a is atmospheric pressure signal (used 10.05 dbar) and ρ is water density (assumed 1.026 g/mL).

The processing of wave data from the PT was done using standard calculation methods as described in [22] and coded in MATLAB by Urs Neumeier, 2003 (http://neumeier.perso.ch/matlab/waves.html). The processing includes the attenuation of pressure variation with depth, which is only applied over a given frequency range to avoid over-amplification of high frequency variations that do not correspond to surface waves, but are instead noise. By default, the correction is applied over the range 0.05-0.33 Hz. The input argument is the water level above the bed (obtained from the PTs) and applied through equation (1). All PTs were deployed at bed level (i.e. elevation of the sensor above the bed is 0 m). From the continuous PT time series, it is possible to identify the start and end of the deployments as the water level goes from zero to positive values at the start and back to zero when the DIST is returned back to shore after one measurement cycle. The full time series (*ca.* 8 min) is used for each deployment to calculate the water depth and wave spectral and zero crossing wave parameters.

Tide elevations are referenced to the Chart Datum (CD) while beach profiles were referenced to the Ordnance Datum (OD). We have used the vertical offshore reference frames software (VORF 2.11) to convert between these two Datums [23; 24]. At the Minsmere Sluice

Journal Pre-proof

location coordinates (52.233, 1.6333) the CD is 1.583 m ± 0.042 m below the OD which is also the vertical datum difference at the landward end of the CSHORE profile. At the seaward end of the CSHORE profile (i.e. where boundary conditions are defined) with location coordinates (52.249, 1.697) the CD is 1.43 m ± 0.100 m below the OD. We have used the CD to OD vertical difference at Minsmere Sluice location to correct the elevations from the bathymetric data and the datum vertical difference at the seaward end of CSHORE profile to correct the astronomical tide levels.

4.2. Numerical simulations with CSHORE model

4.2.1 Model overview

CSHORE is a one-dimensional time-averaged nearshore profile model for predictions of wave height, water level, wave-induced steady currents, and beach profile evolution and stone structural damage progression [15]. CSHORE consists of the following components: a combined wave and current model based on time-averaged continuity, cross-shore and longshore momentum, wave energy or action, and roller energy equations; a sediment transport model for suspended load and bed load; a permeable layer model to account for porous flow and energy dissipation; formulas for irregular wave run-up; a probabilistic model for an intermittently wet and dry zone on impermeable and permeable bottoms for the purpose of predicting wave overwash of a dune and armour layer damage progression, respectively; a drag force model for piles interacting with waves and sand dunes; and a dike erosion model by irregular wave action.

The main CSHORE assumptions are;

- Local longshore uniformity is assumed (i.e. this model cannot be applied to a beach with large longshore variability)

Journal Pre-proof

- Cohesionless uniform sediment size distribution (sand, gravel or stone)
- Hydrodynamic modelling in CSHORE for the sediment transport modelling is limited to the mean and standard deviation of the free surface elevation and depth-averaged cross-shore and longshore velocities on the impermeable and permeable bottoms
- Hydrodynamics at the surf zone and the wet and dry zone are resolved differently. Runup statistics at the wet and dry zone are based on computed mean water surface elevation and its standard deviation at the lower swash-zone. Surf-zone hydrodynamic is calculated resolving the wave action balance (including dissipation and bottom friction) and the phase-averaged momentum integrated to Still Water Surface.

Figure 6 shows the CSHORE convention for obliquely incident irregular waves on a straight shoreline over a permeable slope. The cross-shore coordinate (x) is positive onshore, and the longshore coordinate (y) is positive in the down-wave direction. The depth-averaged cross-shore and longshore velocities are denoted by U and V, respectively. Incident waves are assumed to be unidirectional, with the incident wave angle (θ) relative to the shore normal and uniform in the longshore direction. Wave angle is assumed to be in the range of $|\theta| < 90^{\circ}$ to ensure that the incident waves propagate landward. Wind speed and direction at an elevation of 10 m above the sea surface are denoted by W_{10} and θ_w, respectively. The vertical coordinate (z) is positive upwards; $\bar{\eta}$ is the mean free surface elevation above still water level (SWL); S, the storm tide above $z = 0$; z_b, the bottom elevation; $\bar{h}$, the mean water depth; z_p, the elevation of the lower boundary of the permeable layer; h_p, the vertical thickness of the permeable layer ($z_b - z_p$); and U_p, the instantaneous cross-shore discharge velocity inside the permeable layer. The cross-shore profile of $z_p(x)$ is specified as input, where $h_p = 0$ in the zone of no permeable layer. The lower boundary located at $z = z_p$ is assumed to be impermeable and fixed for simplicity.

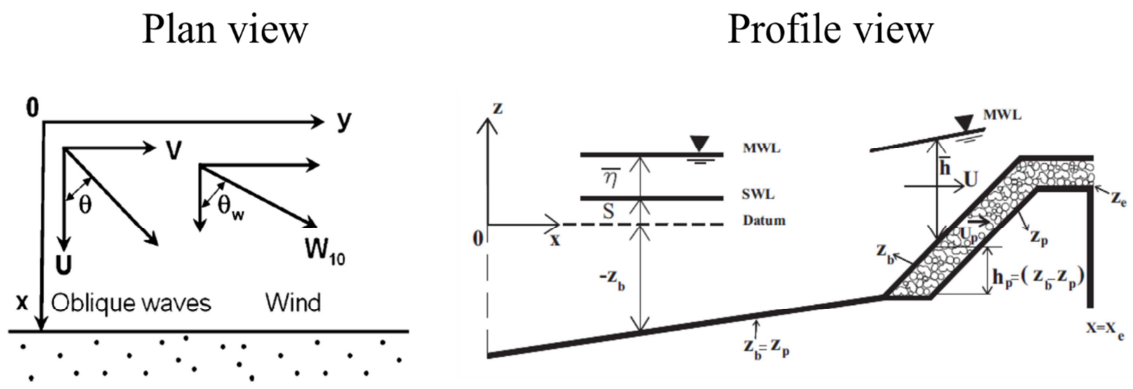

397

398 **Figure 6.** Definition sketch of incident irregular waves and wind on beach of longshore
399 uniformity and permeable layer model (after [15; 18])

400 The combined wave and current model in the wet zone predicts the spatial variations of the
401 hydrodynamic variables used in the following sediment transport formulas for a given beach
402 profile, water level, and seaward wave conditions at $x = 0$. The bottom sediment is assumed
403 to be uniform and characterized by *d50* as the median diameter; w_f, the sediment fall velocity;
404 and *s*, the sediment specific gravity. The sediment particles in the wet zone are always
405 submerged.

406

407 *4.2.2 Longshore suspended and bed load sediment transport formulation in the wet zone*

408 The longshore suspended sediment transport rate q_{sy} is expressed as;

409 $$q_{sy} = \bar{V} V_s \tag{2}$$

410 where, $\bar{V}$ is the time-averaged, depth-averaged velocity in the *y*-direction; V_s is the suspended
411 sediment per unit horizontal bottom area. The mean water depth ($\bar{h}$) and the current velocities
412 ($\bar{U}$ and $\bar{V}$) are computed using the time-averaged continuity and momentum equations (see
413 references in Kobayashi [15]). V_s is estimated by modifying the sediment suspension model
414 by Kobayashi and Johnson [25] as

Journal Pre-proof

Journal Pre-proof

$$V_s = P_s \frac{e_B D_r + e_f D_f}{\rho g (s-1) w_f} (1 + S_b^2)^{0.5}; S_b = \frac{dz_b}{dx} \quad (3)$$

Where P_s is the probability of sediment in suspension; S_b = cross-shore bottom slope; ρ = water density; e_B and e_f = suspension efficiencies for the energy dissipation rates D_r and D_f due to wave breaking and bottom friction, respectively. Use has been made of e_B = 0.005 and e_f = 0.01 as typical values in the computation of berm and dune erosion [15], but the value of e_B is uncertain and should be calibrated in the range of e_B = 0.002–0.01 if V_s is measured.

The energy dissipation rate D_B, caused by wave breaking in Eq. (3), is estimated using the simple formula by Battjes and Stive [26], which was modified by Kobayashi et al. [27] to account for the local bottom slope and to extend the computation to the lower swash zone. The modified formula is expressed as;

$$D_B = \frac{\rho g a_s Q H_B^2}{4T}; \frac{Q-1}{lnQ} = \left(\frac{H_{rms}}{H_m}\right)^2; H_m = \frac{0.88}{k} tanh\left(\frac{\gamma k \bar{h}}{0.88}\right); a_s = \frac{2\pi S_b}{3k\bar{h}} \geq 1 \quad (4)$$

Where, a_s is the slope effect parameter; Q is the fraction of breaking waves; H_B is the breaker height used to estimate D_B; T is the intrinsic wave period given by $T = 2\pi/\omega$ with ω obtained using the dispersion relation for linear waves; H_{rms} is the local root mean square wave height ($\sqrt{8}\sigma_\eta$); σ_η is the standard deviation of the free surface elevation η; H_m is the local depth-limited wave height; k, the wave number; and γ, the empirical breaker ratio parameter. The parameter a_s is the ratio between the wavelength ($2\pi/k$) and the horizontal length ($3\bar{h}/S_b$) imposed by the small depth and relatively steep slope, where the lower limit of a_s = 1 corresponds to the formula by Battjes and Stive [26] who also assumed $H_B = H_m$. The fraction Q is zero for no wave breaking and unity when all waves break. The requirement of $0 \leq Q \leq 1$ implies $H_{rms} \leq H_m$, but H_{rms} can become larger than H_m in very shallow water. When $H_{rms} > H_m$, use is made of $Q = 1$ and $H_B = H_{rms}$. In addition, the upper limit of $\sigma_* = \sigma_\eta/\bar{h}$ is imposed as $\sigma_* \leq 1$ in very shallow water [28]. The breaker ratio parameter g in Eq. (4) is typically in

Journal Pre-proof

the range of γ = 0.5–1.0 but should be calibrated to obtain a good agreement with the measured cross-shore variation of σ_η if such data are available. If no data are available, the value of γ may be taken as a typical value of 0.7 (0.6 for a very gentle slope) [15].

The energy dissipation rate D_f due to bottom friction in Eq. (3) is expressed as;

$$D_f = \frac{1}{2}\rho f_b \overline{U_a^3};\ U_a = (U^2 + V^2)^{0.5} \tag{5}$$

where, f_b is the bottom friction factor, which is of the order of 0.01 on sand beaches but it should be calibrated using longshore current data because of the sensitivity of longshore currents to f_b [15].

The probability of sediment being in suspension (P_s) is calculated as;

$$P_s = \frac{1}{2}erfc\left(\frac{F_s - r_m}{\sqrt{2}}\right) + \frac{1}{2}erfc\left(\frac{F_s + r_m}{\sqrt{2}}\right)\ for\ F_s > 0$$

$$F_s^2 = (R_s^2 - F_m^2);\ R_s^2 = \left[(2/f_b)^{1/3}\, w_f/\sigma_T\right];\ \sigma_T = \sigma_\eta/\bar{h} \tag{6}$$

and P_s =1 for $F_s^2 \leq 0$, where *erfc* is the complementary error function [29]. If $P_s > P_b$, the probability of sediment movement, use is made of $P_s = P_b$ assuming that sediment suspension occurs only when sediment movement occurs. P_b is calculated as;

$$P_b = \frac{1}{2}erfc\left(\frac{F_b - r_m}{\sqrt{2}}\right) + \frac{1}{2}erfc\left(\frac{F_b + r_m}{\sqrt{2}}\right)\ for\ F_b > 0$$

$$F_b^2 = (R_b^2 - F_m^2);\ R_b^2 = \ [2g(s-1)d_{50}\psi_c f_b^{-1}]^{0.5}/\sigma_T \tag{7}$$

and P_b = 1 for $F_b^2 \leq 0$, where ψ_c is the critical Shields parameter, which is taken as ψ_c=0.05 and F_m and r_m are defined as

$$r_m = -(U_* cos\theta + V_* sin\theta);\ F_m = V_* cos\theta - U_* sin\theta;\ U_* = \bar{U}/\sigma_T;\ V_* = \bar{V}/\sigma_T; \tag{8}$$

The longshore bed load sediment transport rates q_{sb} have been devised somewhat intuitively because bed load in the surf zone may never have been measured [15] and is expressed as;

Journal Pre-proof

459 $$q_{by} = bP_b/(g(s-1))\sigma_T^3[V_*(1 + U_*^2 + V_*^2) - 2r_m sin\theta] \quad (9)$$

460

461 *4.2.3 Model inputs*

462 The CSHORE model requires offshore (i.e. unaffected by refraction, shoaling and
463 shadowing) wave data (H_{rms}, T and θ), the Still Water Level (*SWL*), surge levels at the
464 beginning and the end of the simulated period and the profile elevation. We have used the
465 offshore wave data provided by the CEFAS wave rider buoy (Figure 4) as wave forcing at the
466 seaward end of the beach profile. The buoy is deployed at *ca.* 16.8 m water depth relative to
467 Newlyn datum and provides hourly data, including significant wave height, H_s, peak period,
468 T_p, and peak wave direction relative to the Magnetic North, θ_{MN}. At Sizewell site, Magnetic
469 North is approximately 2.716 degrees West (2018). Minsmere Cliff is oriented *ca.* 85
470 degrees, measured clockwise relative to the grid North, and therefore the wave direction
471 using CSHORE convention shown in Figure 6 is obtained as θ [deg]= *85 deg* - θ_N [deg] (i.e.
472 waves propagating at 85 deg clockwise relative to grid North will be perpendicular, $\theta=0$, to
473 shoreline at Minsmere Cliff). We have used the relationship $H_s = 1.42H_{rms}$ *[30]* to convert
474 the wave H_s wave buoy data into the required H_{rms}.

Journal Pre-proof

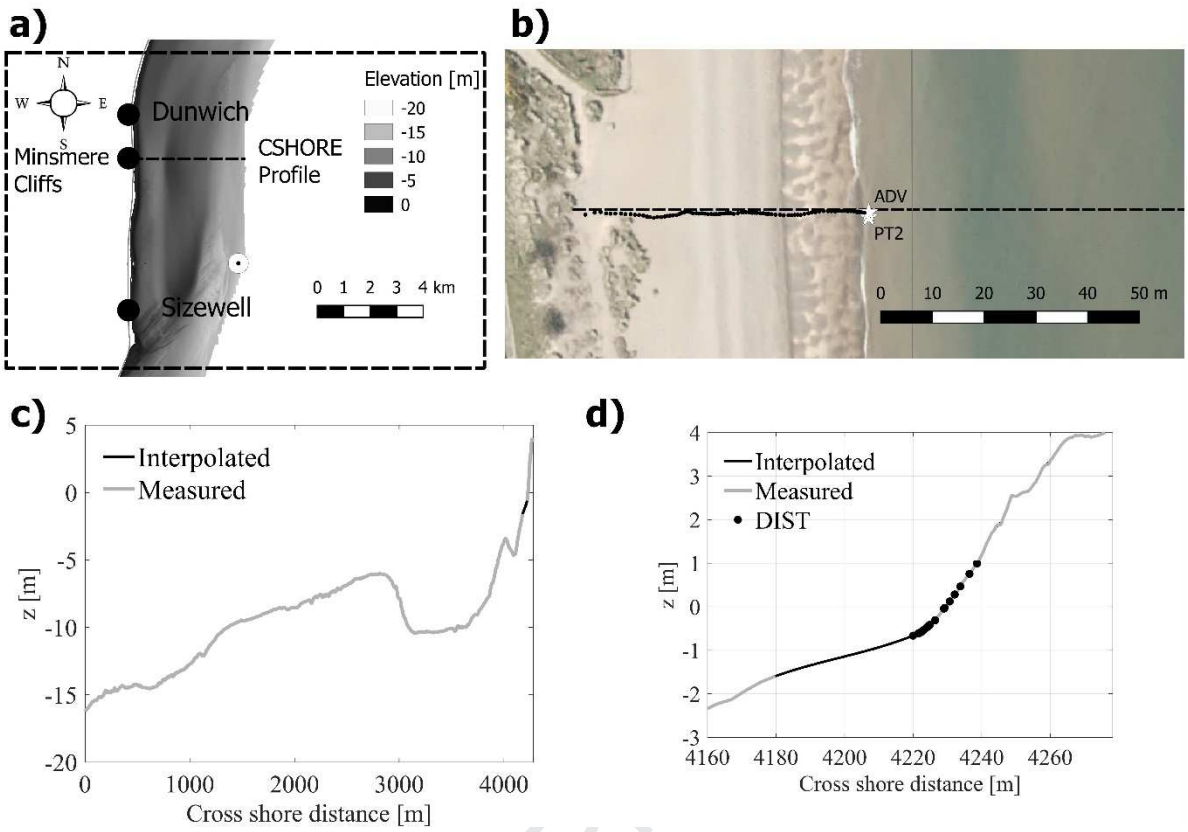

475

476 **Figure 7.** Beach profile used as input for CSHORE simulations: a) the *ca.* 4km long profile
477 runs perpendicular to Minsmere Cliffs, b) beach topographical points location relative to
478 CSHORE profile, c) elevation profile (relative to Newlyn Datum) after merging the
479 bathymetry and topographical data, d) elevation profile zoom in at the location of the DIST
480 deployment locations.

481

482 The CSHORE model requires initial bed elevation profile. The initial elevation profile was
483 obtained by combining the beach profile, measured during the field experiment, and the
484 profile extracted from a recent bathymetry (2017) of the study area. The 1 m resolution
485 bathymetry data (shown in Figure 4) was downloaded from the UKHO Admiralty Marine
486 Data Portal with survey ref: 2017 HI1495 Orford Ness to Southwold Area 4 1m CUBE. The
487 elevation profile was extracted along a perpendicular line to the coast at Minsmere Cliffs of
488 *ca.* 4 km length (see Figure 7a). The seaward end of the profile is at a similar depth than the

Journal Pre-proof

CEFAS wave rider buoy data used as boundary conditions. The elevation provided by the UKHO are referred to the Chart Datum and was converted to the Newlyn Datum using the VORF software (similar to the aforementioned tidal elevation datum transformation). The missing data between the beach profile (Figure 7c) and the profile obtained from the bathymetry data was interpolated using spline interpolation. Most of DIST deployments locations were over the beach measured profile (Figure 7d).

Natural sediments are represented in CSHORE by the single diameter, d_{50} [mm], specific gravity, *s*, and fall velocity, w_f [m/s]. Because CSHORE assumes that natural sediments are mostly made of a single sediment fraction (i.e. sand or gravel) direct comparison with MSG beaches (made of sand and gravel), is not possible. To overcome this limitation we have compared CSHORE simulated sediment transport assuming different d_{50} for suspended and bed load sediment transport. The d_{50} values are obtained from the sediment size analysis of the trapped sediments. The mean d_{50} of the trapped sand fraction is used to simulate the suspended sediment transport and the mean d_{50} of trapped gravel fraction is used to simulate the bed load sediment transport. The fall velocity have been calculated using Soulsby [31] for a temperature of 6°C and water salinity of 35 ppt. Sediment specific gravity used is s = 2.65.

5 RESULTS

5.1 Met-ocean conditions during the observation period

Figure 8 shows the offshore wave conditions during the survey, registered by the Sizewell Waverider buoy (© EDF Energy 2019) and located in 18 m water depth. Waves were approaching from NNE-NE, with maximum offshore significant wave heights of 2.5 m at the start of day 1 and decreasing to 0.7 m by the end of day 2, with a wave peak period between 6

and 8 seconds. The approximate time at which the traps were deployed is indicated by vertical grey bars on the plot.

Figure 9 shows the water elevation changes due to the astronomical tide and the deployment times of the traps. Streamer traps were deployed three times on day 1 and eighteen times on day 2. All three traps collected on day 1 were deployed close to high tide, which was about 2.2 m above Chart Datum. Tide level collected during day 2 increased from 0.9 m at the start of the sampling cycle to 1.9 m at the end. The astronomical tide level differ from the actual water level during the field observation due to the barometric tide and the wind-stress induced tide. The astronomical levels provided by the Admiralty tide tables assumes average atmospheric pressure of 1013 hPa. During day 2 observations, the measured atmospheric pressure during the DIST deployments was 1005 hPa. Due to the barometric tide, astronomical tide levels were increased *ca.* 8 cm. The wind during day 2 was blowing at average speeds less than 4 m/s from the NE and the wind stress induced tide was negligible.

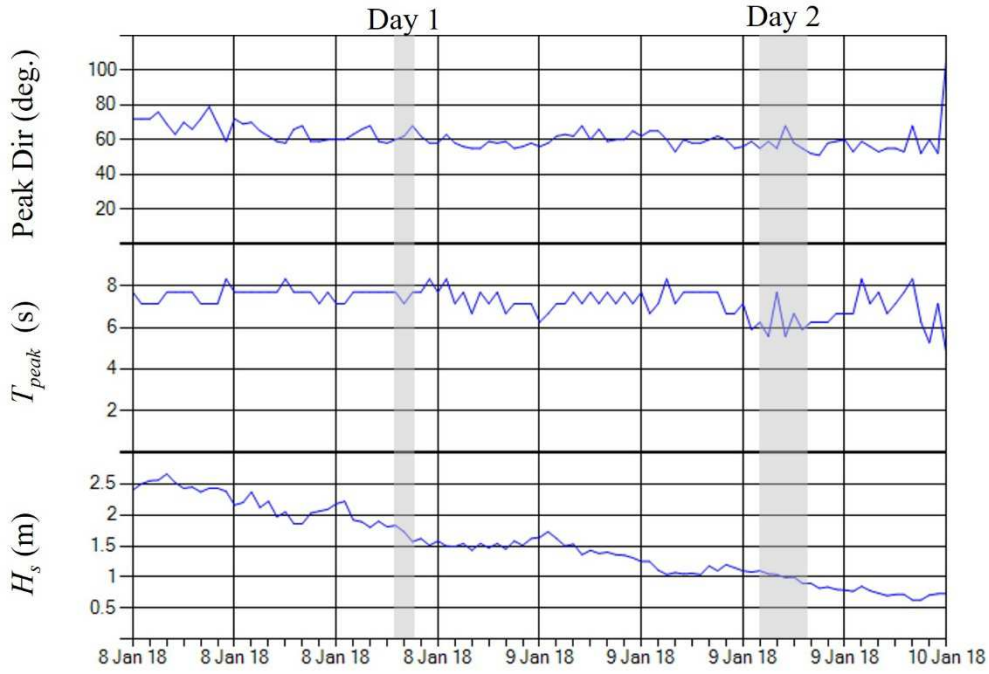

527 **Figure 8.** Time series of offshore wave peak direction, peak period and significant wave
528 height during the field experiment. Vertical grey bars indicated the approximated time during
529 which sampling cycles on Jan 8th (day 1) and 9th (day 2) were performed. Wave direction is
530 given relative to the magnetic North at the location of the Sizewell wave rider buoy.

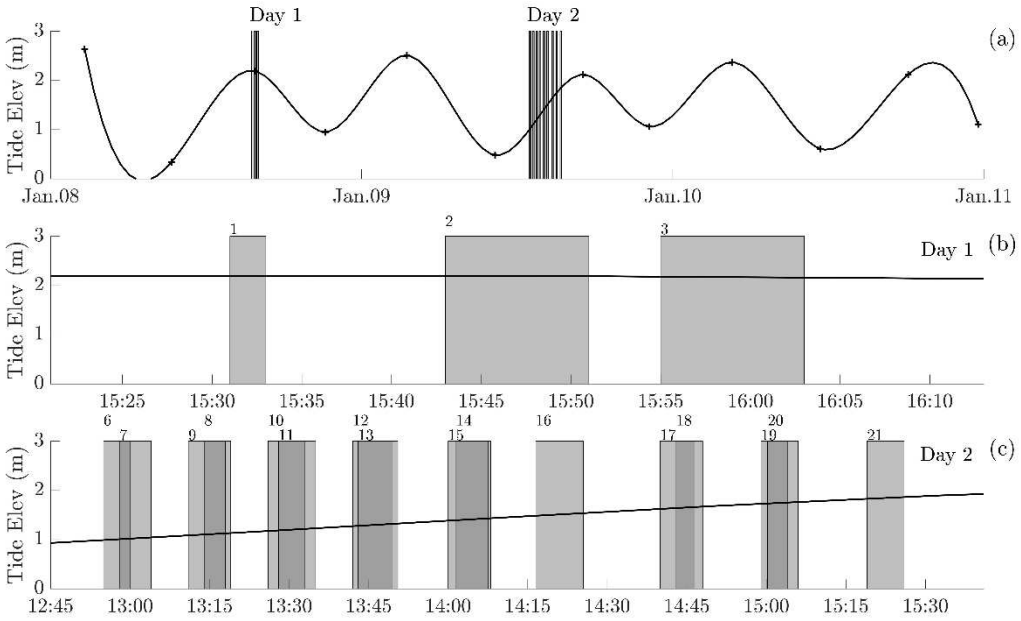

531

532 **Figure 9.** Tide elevation time series during the observation period and trap sampling
533 intervals; (a) Time series has been obtained by fitting a spline function to the predicted low
534 and high tides by the UK Hydrographic office (elevation relative to Chart Datum); (b) and (c)
535 shows the detailed hour (UTC) when traps were deployed during Jan 8th (day 1) and 9th (day
536 2) respectively. The vertical grey bars indicated the time at which traps were deployed and
537 the numbers on the bar's top correspond with the sample unique ID.

538

539 **5.2 Temporal variation of collected depth-integrated total sediment transport**

540 Out of 21 deployments, 19 deployments were valid: the two non-valid deployments were due
541 to the streamer cloth damage, which led to sediment loss, and because material was lost from

Journal Pre-proof

the DIST while recovering it from the water (e.g. when DIST was being transported back to the beach, the trap tilted forward and the incoming waves washed away the trapped sediment from the streamer).

Table 1 shows the temporal variation of the dry weight of the trapped sediments together with the unique ID used for each DIST deployment, the percentages of gravel, sand and fine materials, duration of the deployments, d_{50} and sediment transport rates. The mean sampling duration was 6.4 minutes with a minimum of 2 minutes and a maximum of 9 minutes. The average total trapped dry weight was 1.8 kg, with a minimum of 0.120 kg and a maximum of 4.4 kg. Gravel was the dominant sediment trapped fraction (i.e. percentage of gravel larger than 50%) for 11 of the deployments, sand fraction was dominant for 7 of the deployments and only one deployment (ID = 9), sand and gravel fraction percentages were similar. The average d_{50} was 14.7 mm and 4.0 mm for all samples taken on day 1 (samples 1, 2 and 3) and day 2 (samples 4 to 21), respectively. The maximum d_{50} was 17.4 mm and the minimum of 0.4 mm. The average grain size of the gravel fraction was 9.09 mm ± 2.47 mm, and the average grain size of the sand fraction was 0.73 mm ± 0.26 mm. The detailed sediment size distribution for each sample is available in Appendix A. The average sediment transport rate (i.e. dry weight divided by sampling duration) was higher on day 1 with 33.2 kg/h than on day 2 with 18.8 kg/h. The maximum sediment transport rate was 79 kg/h and the minimum 1 kg/h.

Table 1. Sample ID, dry weight, percentage of gravel, sand and fine fraction, sampling duration, d_{50} and sediment transport rate.

ID	Dry weight (g)	Gravel (%)	Sand (%)	Fine (%)	Duration (min)	d_{50} (mm)	Sed. Trans. Rate (kg/h)
1	2632.02	80.5	19.5	0	2	17.4	79.0
2	227.31	82.2	17.8	0.1	8	12.5	1.7
3	2534.07	95.3	4.6	0	8	14.2	19.0
6	400.37	76.6	23.1	0.2	5	7.6	4.8

Journal Pre-proof

7	653.31	65.9	34.1	0.1	6	5.2	6.5
8	1111.63	84.1	15.8	0.1	5	5.4	13.3
9	119.29	49.6	49.8	0.7	7	1.9	1.0
10	340.69	52.5	47.1	0.3	7	2.5	2.9
11	286.5	43.1	56.7	0.2	7	1.1	2.5
12	909.89	42	57.8	0.2	7.5	0.8	7.3
13	1300.95	35.4	64.5	0.1	7.5	0.5	10.4
14	523.21	17.8	81.9	0.2	6.5	0.4	4.8
15	1515.37	37.6	62.4	0.1	7.5	0.5	12.1
16	4249.75	85.4	14.5	0.1	9	7.7	28.3
17	4406.78	71.7	28.2	0	8	7.7	33.1
18	4392.61	42.8	57.2	0.1	3.5	0.7	75.3
19	3992.19	80.3	19.7	0	5	10.0	47.9
20	1550.64	24.1	75.7	0.1	5.7	0.4	16.2
21	4077.58	83.7	16.2	0	7	11.0	35.0

5.3 Calibration of CSHORE hydrodynamic parameters

Table 2 shows the offshore wave and water level conditions used to simulate the observed water depth, wave height and current velocity during the observations on day 2 (i.e. when DIST were equipped with a PT). The wave angle (shown in Figure 6 with the CSHORE angle convention) was on average 30 deg ± 2.5 deg and, therefore, the longshore current was directed southwards for the whole sampling period. Offshore significant wave height and period were almost constant and H_s = 1.0 m and T_p = 6 s. The water level (i.e. combined astronomical tide and barometric tide) varies from a minimum at the beginning of the sampling cycle of -0.3 m to a maximum of +0.5 m at the end.

Table 2. Deployment ID, date, duration, significant wave height, peak period, direction and water level used as offshore boundary conditions for CSHORE simulations.

ID	Date†	Dur (s)	Hs (m)	Tp (s)	Dir (deg)	Water L. (m OD)
6	09-Jan-2018 12:57:30	300	1.1	6.2	32.5	-0.3

Journal Pre-proof

7	09-Jan-2018 13:01:00	360	1.1	6.1	31.9	-0.3
8	09-Jan-2018 13:16:30	300	1.1	5.8	29.6	-0.2
9	09-Jan-2018 13:14:30	420	1.1	5.8	29.8	-0.2
10	09-Jan-2018 13:29:30	420	1.1	6	30.9	-0.2
11	09-Jan-2018 13:31:30	420	1.1	6.1	31.1	-0.1
12	09-Jan-2018 13:45:45	450	1.1	7.2	32.5	-0.1
13	09-Jan-2018 13:46:45	450	1.1	7.3	32.6	0
14	09-Jan-2018 14:04:45	390	1.1	7	28.6	0.1
15	09-Jan-2018 14:03:45	450	1.1	7	29	0.1
16	09-Jan-2018 14:21:00	540	1	6	22.6	0.2
17	09-Jan-2018 14:44:00	480	1	6.2	28.2	0.3
18	09-Jan-2018 14:44:45	210	1	6.2	28.4	0.3
19	09-Jan-2018 15:01:30	300	1	6.5	30.9	0.4
20	09-Jan-2018 15:03:07	345	1	6.5	31.1	0.4
21	09-Jan-2018 15:22:30	420	1	6.2	32.6	0.5

[†]Date is the average date at the start and end of the DIST sampling

Figure 10 shows the comparison between the simulated and observed water depth, H_{rms} and longshore velocity for all the simulated events listed in Table 2. The mean ratio of the measured H_{rms} and water depth at the DIST deployment location was 0.92 ± 0.23 and, therefore, we have use $\gamma = 0.92$ as the breaker ratio parameter, which is well within the typical expected values ($\gamma = 0.5–1.0$) [15]. The simulated mean water depths, $\bar{h}$, are in good agreement (root mean square error is 0.0762 m) with the observed mean water depth at the fix location of PT2 and the DIST deployment locations (Figure 10). The root mean square error for the H_{rms} at the DIST locations is 0.034 m and 0.32 m at the PT2 fixed location: H_{rms} at DIST locations are predicted with a mean factor of 0.98 ± 0.1 while H_{rms} at PT2 fixed

location are over predicted by a mean factor of 1.6 ± 0.42. The friction factor, f_b = 0.035, was used to fit the longshore velocities, *V*, observed at the fixed ADV location. Assuming that velocities measured at a fixed location are of the same order as the depth averaged longshore velocity, the observed *V* velocities were predicted by a mean factor of 1.06 ± 0.19.

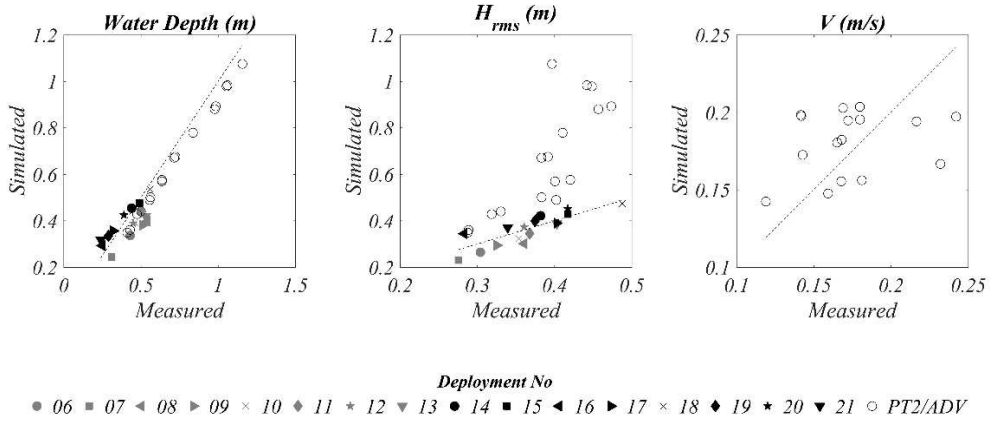

Figure 10. Simulated vs measured mean water depth, H_{rms} and longshore velocity, *V*. Longshore measured velocity is at a fixed depth while simulated velocities are depth averaged.

5.4 Simulated vs measured suspended sediment transport

We have used *d50* = 0.73 mm (i.e. mean sediment size of trapped sand fraction) to represent the natural sediment on the beach and to compare it with the suspended sediment transport rate. We first tried the typical values used in the computation of berm and dune erosion [15], e_B = 0.005 and e_f =0.01 (i.e. suspension efficiencies for the energy dissipation rates due to wave breaking and bottom friction, respectively), however, this underestimated the observed suspended longshore sediment transport by several orders of magnitude. Kobayashi [15] indicated that the value of e_B is uncertain and should be calibrated in the range of e_B = 0.002–0.01 if V_s is measured. Using the maximum recommended value $e_B = e_f$ = 0.01 the observed

suspended sediment transport rate was still under-predicted. Only when the e_B and e_f efficiency values were increased by a factor of 31.5 (e_B = e_f = 0.315) the maximum recommended value was there good agreement between the observed and simulated suspended sediment transport (Figure 11). The suspended sediment transport measured during DIST deployment num. 18 was *ca.* 2.8 times higher than the simulated one. Figure 11 also shows the probability of natural sediment of *d50* = 0.73 mm, being set in motion, P_b, and in suspension, P_s. For all DIST deployments $P_b = P_s$, and varies from 0.57 to 0.9.

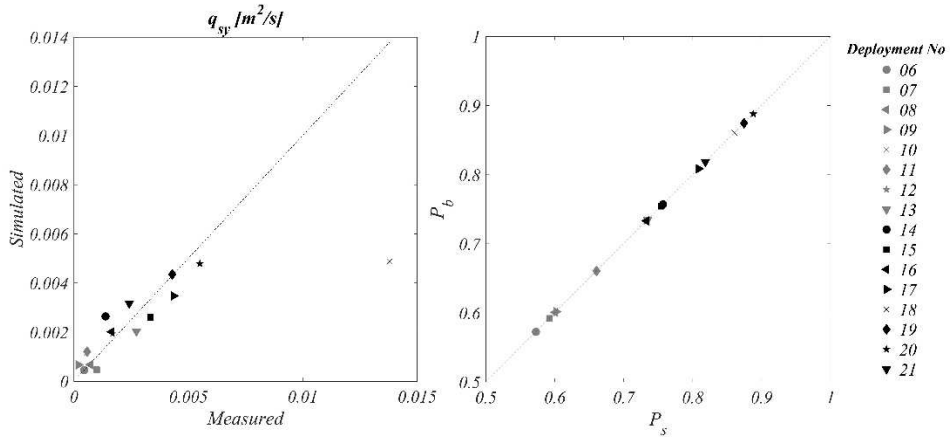

Figure 11. Measured and simulated suspended sediment transport for all DIST deployments assuming $e_B = e_f = 0.315$. The assumption that the sand fraction was mostly transported as suspended sediment transport is well supported by the probability of sediment being in suspension, P_s, being larger than the probability of setting the sediment in motion, P_b. Note: When $P_s > P_b$ CSHORE assumes then that $P_b = P_s$.

5.5 Simulated vs measures bed load sediment transport

Journal Pre-proof

620 Combining the measured bed load sediment transport rate, $\hat{q}_{by}$, mean water depth, $\hat{h}$, $\widehat{\sigma_\eta}$ and
621 $\widehat{T_p}$ together with the simulated $\bar{U}$, $\bar{V}$, θ, σ_T, P_b, P_s we have estimated bed load parameter $\hat{b}$
622 for each DIST deployment on day 2 (Table 3). We have expressed $\hat{q}_{by}$ as volumetric
623 sediment flux rate per unit of across shore length, by dividing the dry weight of the gravel
624 fraction by the sand density, ρ = 2650 kg/m^3, the duration of the sampling in seconds, and the
625 DIST width (0.25 m). The depth integrated and time averaged $\bar{U}$ and $\bar{V}$ have been extracted
626 from the CSHORE simulations at the DIST cross-shore locations. The values of P_s and P_b
627 have been obtained from Eq. (6) and (7) assuming *d50* = 9.09 mm (i.e. the mean *d50* of the
628 trapped gravel fraction on day 2). We have obtained the estimated bed load parameter, $\hat{b}$, by
629 dividing $\hat{q}_{by}$ by $P_b/(g(s\text{-}1))\sigma_T^3[V_*(1+U_*^2+V_*^2)-2r_m sin\theta]$. We have considered valid
630 deployments only those for which the probability of the sediment being set in motion were
631 larger than 0. By imposing this condition, only 9 deployments out of the 16 DIST
632 deployments (56%) done on day 2 were considered valid. The mean $\hat{b}$ value was 0.509 ±
633 0.35 (Figure 12) but data suggest that there is a 100% uncertainty on this value, and therefore
634 $\hat{b}$ varies between 0.254 to 1.018 (i.e. 99% of the data fall within this range).

635

Journal Pre-proof

Journal Pre-proof

636

637

638 **Table 3.** Measured longshore bed load sediment transport rate, $\hat{q}_{by}$, mean water depth, $\hat{h}$, $\widehat{\sigma_\eta}$
639 , $\widehat{T_p}$ and $\widehat{\sigma_T}$ together with the simulated $\bar{U}$, $\bar{V}$, θ, P_b, P_s and estimated bed load parameter $\hat{b}$ for
640 each DIST deployment on day 2 assuming *d50* = 9.09 mm.

ID	$\hat{q}_{by}$ [m^2/s/m]	$\hat{h}$ [m]	$\widehat{\sigma_\eta}$ [m]	$\widehat{Tp}$ [m]	$\bar{U}$ [m/s]	$\bar{V}$ [m/s]	θ [rad]	$\widehat{\sigma_T}$	P_b	P_s	C†	$\hat{b}$
6	1.503E-03	0.43	0.14	4.53	-0.14	0.14	0.11	0.53	0.02	0.02	0.26	NaN
7	1.934E-03	0.31	0.11	28	-0.18	0.15	0.09	0.07	0	0	27.85	NaN
8	3.835E-03	0.54	0.15	8.36	-0.15	0.16	0.11	0.31	0	0	0.7	NaN
9	1.920E-04	0.51	0.15	5.52	-0.15	0.16	0.11	0.47	0.21	0.21	0.37	0.4
10	6.120E-04	0.46	0.15	5.24	-0.18	0.2	0.11	0.49	0.17	0.17	0.46	1.06
11	4.390E-04	0.5	0.15	6.63	-0.17	0.2	0.11	0.39	0.34	0.34	0.66	0.55
12	1.225E-03	0.45	0.15	6.19	-0.24	0.22	0.1	0.42	0.57	0.57	0.76	0.64
13	1.501E-03	0.53	0.18	5.78	-0.23	0.23	0.11	0.53	1	1	0.49	0.32
14	3.000E-04	0.44	0.17	5.09	-0.24	0.24	0.1	0.57	1	1	0.48	0.05
15	2.014E-03	0.49	0.17	7.62	-0.23	0.24	0.1	0.38	1	1	0.96	0.61
16	9.748E-03	0.25	0.12	6.68	-0.28	0.2	0.07	0.31	0	0	1.35	NaN
17	1.107E-02	0.32	0.15	7.18	-0.26	0.26	0.1	0.36	0	0	1.39	NaN
18	1.032E-02	0.56	0.26	6.87	-0.24	0.29	0.12	0.65	0.93	0.93	0.54	1.23
19	1.753E-02	0.29	0.14	6.9	-0.3	0.27	0.1	0.35	0	0	1.73	NaN
20	1.752E-03	0.39	0.17	5.74	-0.23	0.29	0.11	0.51	1	1	0.81	0.27
21	1.250E-02	0.24	0.13	6.44	-0.21	0.26	0.11	0.35	0	0	1.37	NaN

† C = $[V_*(1 + U_*^2 + V_*^2) - 2r_m sin\theta]$ from Eq. (9)

641

642

Journal Pre-proof

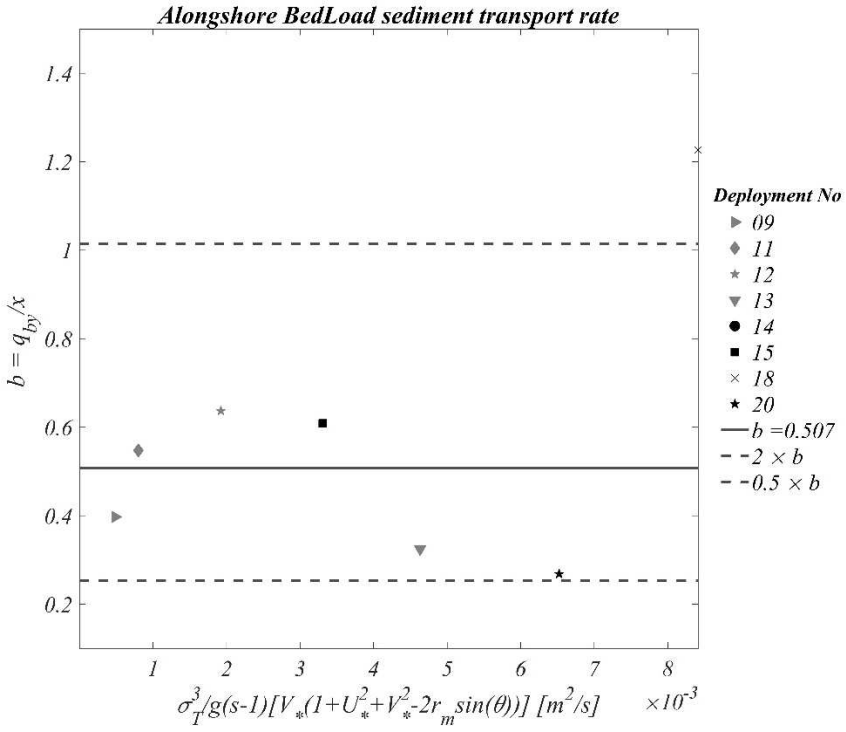

643

644 **Figure 12.** Observed bedload transport is proportional to longshore wave energy flux within
645 a factor two uncertainty. Only DIST deployments for which the probability of the sediment of
646 d50 = 9.09 mm being set in motion were considered valid (i.e. 56% of all observations).
647 Dashed lines shows factor two uncertainty around mean estimated bedload parameter, *b*.

648

649 **6 DISCUSSION**

650 We have conducted a field observation of sediment transport for a MSG beach, with a new
651 streamer trap designed to trap the depth integrated, combined suspended and bed load
652 transport. To assess the validity of the new measurement device we have compared the
653 observed suspended and bed load sediment transport with the CSHORE depth integrated
654 model.

655 All the valid 16 deployments undertaken during day 2, when wave energy and water levels at
656 the trap deployment locations were also recorded (Table 3), were done at mean water depth

Journal Pre-proof

657 between 0.24 m to 0.56 m (i.e., they were always in the wet zone, where the CSHORE
658 sediment transport formulation presented in section 4.2.2 is applicable. CSHORE assumes
659 that the natural sediment size is well sorted and is mostly made of sand, or gravel or stones,
660 but has not been tested yet for MSG beaches. We have compared CSHORE simulated
661 suspended and bed load sediment transport with the observed sand fraction (*d50* = 0.73 mm)
662 and gravel fraction (*d50* = 9.09 mm) sediment transport rates. The assumption that the sand
663 fraction was transported as suspended sediment is supported by the estimated P_s being larger
664 than P_b for all 16 deployments (Figure 11) with P_s = 0.56 to 0.9. On the contrary, the
665 assumption that the gravel fraction was transported as a bed load is not supported, as the
666 estimated P_s were larger than P_b for all 16 deployments (Table 3). In this context, it was
667 expected that the longshore suspended transport Eq. (2) will produce a better fit than the
668 longshore bed load sediment transport Eq. (9) to the observations.

669 The simulated $\bar{h}$, H_{rms} and $\bar{V}$ were predicted by a factor *ca.* 1 (Figure 10) using the breaking
670 ratio parameter γ = 0.92 and bottom friction facto f_b = 0.035, which are well within the range
671 of expected values for these parameters [15; 32].

672 The observed suspended sediment transport is in good agreement with that predicted by Eq.
673 (2) if the efficiency of wave breaking is increased to e_B = 0.315 (Figure 11). Kobayashi [15]
674 indicated that the value of e_B is uncertain and should be calibrated in the range of e_B = 0.002–
675 0.01 if V_s is measured. This recommended range for e_B is based on observations at a wave
676 basin for *d50* = 0.15 mm, were V_s was measured inside and outside the surf zone but not at
677 the location were maximum $\bar{V}$ was simulated near the mean still water shoreline [33].
678 Maximum e_B (0.01) was needed to improve the agreement in the outer surf zone with the
679 observed V_s by Farhadzadeh et al. [33]. The DIST deployment locations are close to the
680 mean still water shoreline, where maximum longshore velocities are estimated by CSHORE
681 simulations. We found that e_B needed to be increased to 0.315 to get a good agreement with

Journal Pre-proof

682 the observed longshore suspended sediment transport rate (Figure 11). It is noted that, the
683 recommended e_B values by Kobayashi [15] are mostly based on flume or wave-basin
684 experiments of uniform sediment material, where dominant wave breaking mode was
685 spilling, whilst we have made the observations under plunging breaking mode. The P_s values
686 ranges from 0.56 to 0.9, which is similar to the values reported by Kobayashi et al. [34] of
687 0.45 to 0.88 for a large flume experiment with *d50* = 0.23 mm. The presence of gravel,
688 combined with the plunging breaking, seems to increase by a factor of 30 the efficiency of
689 wave breaking on getting sediment transported as suspended sediment.

690 As expected, the agreement between the observed bed load sediment transport and that
691 predicted by Eq. (9) is not as good as for the suspended sediment transport (Table 3). Based
692 on the P_b and P_s estimated values for the observed wave energy and water level at the DIST
693 deployment locations, only 56% of the samples were considered valid. The remaining 44% of
694 samples were considered not valid because the gravel sediment fraction was unlikely to be in
695 motion or suspension ($P_s = P_b = 0$) and, therefore, the amount of trapped sediment was
696 unlikely to be related with longshore sediment transport. For the remaining valid 56% of the
697 observations, the predicted probabilities of sediment movement and suspension are the same
698 and in the range of 0.17 to 1.0, suggesting that suspension of medium size gravel (*d50* = 9.09
699 mm) occurs when its movement is initiated in these field observation. The mean bed load
700 parameter, $\hat{b}$, estimated from the observations was 0.509 with a 100% uncertainty. This value
701 is several order of magnitude larger than the maximum bed load parameter 0.003 used by
702 Kobayashi and Jung [32] to simulate beach erosion and recovery close to the still water
703 shoreline of a sandy beach. While a 100% uncertainty is not un-usual when working with
704 bedload transport, we believe that this uncertainty is mostly due to the assumption of the
705 coarser sediment fraction been transported as bedload not been a good assumption as
706 suggested by the high Ps values. Other problems such as scouring, trapping and anchoring

Journal Pre-proof

might be also affecting the measurements. More field observations of bedload sediment transport are needed on MSG beaches under plunging waves to fill this data gap and to offer additional statistics for comparing against the theory.

7 CONCLUSIONS

Observations of the depth integrated and time averaged sediment transport were measured at 19 locations inside the surf zone on a MSG beach. These were taken under moderate offshore wave energy conditions and varying water levels, and these are presented and analysed to examine the performance of a new portable streamer trap.

The proposed Depth Integrated Streamer Trap (DIST) is inspired by the design described by Kraus [6], but avoids errors associated with fitting a vertical distribution to a discrete number of elevations by using a streamer trap mouth big enough to capture all sediment at depths where it is safe to deploy the device (1 m mean water depth). Stability of the device is achieved by gravity (i.e. combined weight of the device and operator) instead of thrusting the legs of the frame into the seabed. The proposed design mitigates some of the known limitations of existing sediment trap devices. Bed disturbance (scour) around the trapping element is minimized by use of a reticulated base that quickly settles into the sea bed. The trap is designed to measure the combined bed load and suspended load sediment transport during short (5 to 10 minutes) deployments. The device is heavy enough (46 kg) to provide stability, but can be transported by two people. The trap is easily operated with minimum sample handling in the field. The trap mouth, streamer dimension and mesh size have been made large enough to avoid local acceleration or deceleration of flow, but we have not measured the trap hydraulic resistance and sediment trapping characteristics. The weakest

Journal Pre-proof

731 mechanical element of the device is the streamer sieve mesh. To avoid the streamer from
732 breaking, the authors have subsequently replaced the original polyester mesh by a stainless
733 steel mesh of same mesh size.

734 The observed longshore suspended and bed load transport has been compared with the depth
735 integrated and time averaged CSHORE numerical model. The CSHORE model formulation
736 has been formulated for beaches of uniform sediment size and, therefore, a one to one
737 agreement was not expected with the observations undertaken for the MSG beach of
738 Minsmere. The predicted probabilities of sediment movement and suspension are the same
739 ($P_b = P_s$) for all the valid deployments, suggesting that suspension of coarse size sand ($d50$ =
740 0.73 mm) and medium size gravel ($d50$ = 9.09 mm) occurs when its movement is initiated. In
741 this context, the CSHORE formulation for longshore suspended sediment transport was in
742 good agreement with 99% of the observations, if the efficiency of wave breaking was
743 increased by an order of magnitude relative to the maximum e_B (0.01) recommended for the
744 outer surf zone. This good agreement suggests that the traps are capturing the longshore
745 sediment transport (i.e. trapped sediment is proportional to the wave energy flux) and that
746 wave breaking is more effective on MSG beaches than in uniform size beaches. The observed
747 bed load sediment transport was considered valid only on 56% of the 16 DIST deployments
748 (i.e. trapped sediment unlikely to be associated with longshore bed load sediment transport).
749 The estimated bed load parameter from observations, $\hat{b}$, varies between 0.254 to 1.018 (i.e.
750 99% of the valid data fall within this range) which is larger than the maximum b = 0.003 used
751 to predict beach recovery by Kobayashi and Jung [32].

752 Accurate observation of combined bed load and suspended sediment transport inside the surf
753 zone on a MSG beach are challenging to make and there are not many devices at the disposal
754 of the Coastal Engineering community to choose from. With this work we have proposed and
755 tested a new portable device to fill this gap. The combined use of a numerical model able to

Journal Pre-proof

accurately reproduce the hydrodynamic under field conditions with the proposed Depth Integrated Streamer Trap and auxiliary wave energy and current velocity measurement devices has the potential to improve our understanding of sediment transport on MSG beaches.

The presented data represented only ~21 discrete sample events of up to 10 min duration. A larger number of samples is yet still needed to overcome the relatively low recovery data (56% for bedload observation) and to characterize the inherent variability of non-cohesive sediment suspensions in the surf zone under turbulent flow conditions. This would offer additional statistics for comparing against the theory.

ACKNOWLEDGEMENTS

This research was funded by the UK Natural Environment Research Council (NE/M004996/1; BLUE-coast project). Authors publishes with permission of the Executive Director of the British Geological Survey, UKRI. The authors would like to acknowledge the support provided by Chris Williams and Daniel Parks with the streamer trap field survey, Matthew Kirkham with the sediment sample size analysis and Dr Christopher Stokes, Mr Aaron Barrett, Mr Oli Bilson and Mr Ben Hall from Plymouth University with the topographic and ADV data collection. The authors would like to acknowledge the two anonymous reviewers for their positive and detailed revisions that has significantly improved this manuscript.

REFERENCES

[1] Buscombe, D. and Masselink, G., 2006. Concepts in gravel beach dynamics. Earth-Science Reviews, 79(1-2): 33-52.

[2] Bergillos, R.J., Masselink, G. and Ortega-Sánchez, M., 2017. Coupling cross-shore and longshore sediment transport to model storm response along a mixed sand-gravel coast under varying wave directions. Coastal Engineering, 129: 93-104.
[3] Dean, R.G., 2003. Beach nourishment: theory and practice, 18. World Scientific Publishing Company.
[4] Hinkel, J. et al., 2014. Coastal flood damage and adaptation costs under 21st century sea-level rise. Proceedings of the National Academy of Sciences, 111(9): 3292-3297.
[5] Van Wellen, E., Chadwick, A.J. and Mason, T., 2000. A review and assessment of longshore sediment transport equations for coarse-grained beaches. Coastal Engineering, 40(3): 243-275.
[6] Kraus, N.C., 1987. Application of portable traps for obtaining point measurements of sediment transport rates in the surf zone. Journal of coastal Research: 139-152.
[7] Wang, P., 1998. Longshore sediment flux in water column and across surf zone. Journal of waterway, port, coastal, and ocean engineering, 124(3): 108-117.
[8] Wang, P., Kraus, N.C. and Davis Jr, R.A., 1998. Total longshore sediment transport rate in the surf zone: field measurements and empirical predictions. Journal of Coastal Research: 269-282.
[9] Kumar, V.S., Anand, N., Chandramohan, P. and Naik, G., 2003. Longshore sediment transport rate—measurement and estimation, central west coast of India. Coastal Engineering, 48(2): 95-109.
[10] Tonk, A. and Masselink, G., 2005. Evaluation of Longshore Transport Equations with OBS Sensors, Streamer Traps, and Fluorescent Tracer. Journal of Coastal Research: 915-931.
[11] Allen, J.R., 2012. Field measurement of longshore sediment transport: Sandy Hook, New Jersey, USA. Journal of Coastal Research, 1(3): 231-240.
[12] Dawe, I.N., 2006. Longshore sediment transport on a mixed sand and gravel lakeshore, University of Canterbury, Christchurch, New Zealand, 364 pp.
[13] Chadwick, A., 1989. Field measurements and numerical model verification of coastal shingle transport. Advances in Water Modelling and Measurement: 381-402.
[14] Bray, M., Workman, M., Smith, J. and Pope, D., 1996. Field measurements of shingle transport using electronic tracers. Proceedings of the 31st MAFF Conference of River and Coastal Engineers, Loughborough, UK, 1-10.
[15] Kobayashi, N., 2016. Coastal sediment transport modeling for engineering applications. Journal of Waterway, Port, Coastal, and Ocean Engineering, 142(6): 03116001.
[16] Wang, P. and Kraus, N.C., 1999. Longshore sediment transport rate measured by short-term impoundment. Journal of waterway, port, coastal, and ocean engineering, 125(3): 118-126.
[17] Rosati, J.D. and Kraus, N.C., 1989. Development of a portable sand trap for use in the nearshore. Coastal Engineering Research Center Vicksburg MS, 181 pp.
[18] Payo, A., Kobayashi, N. and Yamada, F., 2009. Suspended Sand Transport along Pier Depression. Journal of Waterway, Port, Coastal, and Ocean Engineering, 135(5): 245-249.
[19] Katori, S., 1983. Measurement of sediment transport by streamer trap. Report of the 7th Cooperative Field Investigation, Nearshore Environment Research Center, Report No, 17: 110-117.
[20] Folk, R.L., 1954. The Distinction between Grain Size and Mineral Composition in Sedimentary-Rock Nomenclature. The Journal of Geology, 62(4): 344-359.
[21] Pye, K. and Blott, S.J., 2006. Coastal processes and morphological change in the Dunwich-Sizewell area, Suffolk, UK. Journal of Coastal Research, 22(3): 453-473.
[22] Tucker, M. and Pitt, E., 2001. Waves in ocean engineering, Vol. 5 of Elsevier ocean engineering book series. Elsevier Amsterdam, pp. 548.
[23] Turner, J.F., Iliffe, J.C., Ziebart, M.K., Wilson, C. and Horsburgh, K.J., 2010. Interpolation of Tidal Levels in the Coastal Zone for the Creation of a Hydrographic Datum. Journal of Atmospheric and Oceanic Technology, 27(3): 605-613.

Journal Pre-proof

[24] Iliffe, J.C., Ziebart, M.K., Turner, J.F., Talbot, A.J. and Lessnoff, A.P., 2013. Accuracy of vertical datum surfaces in coastal and offshore zones. Survey Review, 45(331): 254-262.

[25] Kobayashi, N. and Johnson, B.D., 2001. Sand suspension, storage, advection, and settling in surf and swash zones. Journal of Geophysical Research: Oceans (1978–2012), 106(C5): 9363-9376.

[26] Battjes, J. and Stive, M., 1985. Calibration and verification of a dissipation model for random breaking waves. Journal of Geophysical Research: Oceans, 90(C5): 9159-9167.

[27] Kobayashi, N., Zhao, H. and Tega, Y., 2005. Suspended sand transport in surf zones. Journal of Geophysical Research: Oceans, 110(C12).

[28] Kobayashi, N., Herrman, M.N., Johnson, B.D. and Orzech, M.D., 1998. Probability distribution of surface elevation in surf and swash zones. Journal of Waterway, Port, Coastal, and Ocean Engineering, 124(3): 99-107.

[29] Press, W.H., Teukolsky, S.A., Vetterling, W.T. and Flannery, B.P., 2007. Numerical recipes 3rd edition: The art of scientific computing. Cambridge University Press, New York, USA.

[30] Thornton, E.B. and Guza, R., 1983. Transformation of wave height distribution. Journal of Geophysical Research: Oceans, 88(C10): 5925-5938.

[31] Soulsby, R., 1997. Dynamics of marine sands: a manual for practical applications. Thomas Telford.

[32] Kobayashi, N. and Jung, H., 2012. Beach erosion and recovery. Journal of Waterway, Port, Coastal, and Ocean Engineering, 138(6): 473-483.

[33] Farhadzadeh, A., Kobayashi, N. and Gravens, M.B., 2011. Effect of breaking waves and external current on longshore sediment transport. Journal of Waterway, Port, Coastal, and Ocean Engineering, 138(3): 256-260.

[34] Kobayashi, N., Payo, A. and Schmied, L., 2008. Cross-shore suspended sand and bed load transport on beaches. Journal of Geophysical Research: Oceans, 113(C7): C07001.

Journal Pre-proof

Journal Pre-proof

- Measurement of the longshore sediment transport rate in the surf zone remains one of the great challenges in coastal engineering and coastal sciences.
- Streamer traps for sand beaches have proven useful in the past, but are not suitable for Mixed Sand and Gravel (MSG) beaches.
- This paper describes a portable depth integrated, streamer trap designed to measure the depth-integrated combined bed load and suspended longshore sediment transport on MSG beaches.
- The device has been tested in the field under moderate wave conditions at Minsmere, UK.
- The data suggest that the empirical efficiency of wave breaking and bed load parameter are several orders of magnitude larger than that previously observed for uniform fine sand values

Journal Pre-proof

Journal Pre-proof

Declaration of interests

☒ The authors declare that they have no known competing financial interests or personal relationships that could have appeared to influence the work reported in this paper.

☐The authors declare the following financial interests/personal relationships which may be considered as potential competing interests:

Declarations of interest: none

Journal Pre-proof